Ab Initio and Kinetic Modeling Studies of Formic Acid Oxidation.

Paul Marshall[1] and Peter Glarborg[2]

[1]*Department of Chemistry and Center for Advanced Scientific Computing and Modeling (CASCaM), University of North Texas, Denton, 1155 Union Circle #305070, Texas 76203–5017*

[2]*Department of Chemical and Biochemical Engineering, Technical University of Denmark, DK-2800 Kgs. Lyngby, Denmark*

Preferred colloquium:

Total length of paper: 5949 words

Method of determination: Method 1

Equivalent lengths:

- Main text: 3413 words
- References: 1151 words
- Tables: 612 words
- Figures: 773 words (5 figures in 67×45 mm)

Supplemental material available

Ab Initio and Kinetic Modeling Studies of Formic Acid Oxidation.

Paul Marshall[1] and Peter Glarborg[2]

[1] *Department of Chemistry and Center for Advanced Scientific Computing and Modeling (CASCaM), University of North Texas, Denton, 1155 Union Circle #305070, Texas 76203–5017*

[2] *Department of Chemical and Biochemical Engineering, Technical University of Denmark, DK-2800 Kgs. Lyngby, Denmark*

A detailed chemical kinetic model for oxidation of formic acid (HOCHO) in flames has been developed, based on theoretical work and data from literature. Ab initio calculations were used to obtain rate coefficients for reactions of HOCHO with H, O, and HO_2. Modeling predictions with the mechanism have been compared to the experimental results of de Wilde and van Tiggelen [Bull. Soc. Chim. Belges 77 (1968) 67-76] who measured the laminar burning velocities for HOCHO flames over a range of stoichiometries and dilution ratios. The modeling predictions are generally satisfactory. The governing reaction mechanisms are outlined based on calculations with the kinetic model. Formic acid is consumed mainly by reaction with OH, yielding OCHO, which dissociates rapidly to CO_2 + H, and HOCO, which may dissociate to CO + OH or CO_2 + H, or react with H, OH, or O_2 to form more stable products. The branching fraction of the HOCHO + OH reaction, as well as the fate of HOCO, determines the oxidation rate of formic acid. At lower temperatures HO_2, formed from HOCO + O_2, is an important chain carrier and modeling predictions become sensitive to the HOCHO + HO_2 reaction.

Keywords: formic acid, ab initio calculations, kinetic model, flame speed

Introduction

Organic acids are among the pollutants of urban and rural atmospheres and contribute to acid rain formation [1, 2]. Emissions of monocarboxylic acids have been detected from IC engines [3, 4] and they are known to form in biomass pyrolysis [5]. The simplest of these acids is formic acid (HC(O)OH, or here HOCHO), which has been identified as an intermediate in oxidation of oxygenated hydrocarbons such as methanol [6] and DME [7]. The detection of carboxylic acid emissions from engines has prompted interest in the combustion chemistry of these components and their formation in laminar premixed hydrocarbon flames has been investigated both experimentally [8] and in terms of chemical kinetic modeling [9].

Detailed reaction subsets for HOCHO formation and oxidation have been proposed by Marinov [10], Fisher et al. [7] and, more recently, by Battin-Leclerc et al. [9]. Battin-Leclerc et al. conclude that formic acid in hydrocarbon flames is mostly formed from the addition of OH radicals to formaldehyde, followed by the elimination of a hydrogen atom [9], CH_2O + OH (+M) $\rightleftharpoons$ $HOCH_2O$ (+M), $HOCH_2O$ (+M) $\rightleftharpoons$ HOCHO + H (+M). This mechanism is similar to what has been proposed earlier for acetaldehyde [11]. Addition of OH to acetylene may also prove to be a source of formic acid. Alzueta et al. [12] identified the chain-propagating sequence $C_2H_2 \xrightarrow{+OH} C_2H_2OH \xrightarrow{+O_2} OCHCHO + OH$ as important for onset of reaction for C_2H_2 at atmospheric pressure and temperatures above 700 K. Interest in

this oxidation pathway for atmospheric chemistry has motivated experimental and theoretical work on the $C_2H_2 + OH + O_2$ reaction at low temperature. Hatakeyama et al. [13] showed in smog-chamber experiments that the reaction generates formic acid (+HCO), as well as glyoxal (+OH). The yield of formic acid in the $C_2H_2OH + O_2$ reaction at lower temperatures has been determined to be in the range 30-50% [13–15]. Since the branching fraction for the reaction is not expected to be strongly temperature dependent, it is possibly a source of formic acid also at combustion conditions, particularly at increased pressure.

Despite the interest in formic acid as the simplest monocarboxylic acid and as an intermediate in and possible pollutant from combustion, work on its gas-phase chemistry at elevated temperatures is scarce. The thermal decomposition of HOCHO has been characterized in batch reactor [18, 19] and flow reactor [19] experiments at intermediate temperatures, and in shock tubes [20–23] at high temperatures. However, the oxidation of formic acid is poorly characterized experimentally. Bone and Gardner [24] conducted static reactor experiments on formic acid oxidation at temperatures between 613 and 743 K, but reported no quantitative results. At higher temperatures, data on the gas-phase oxidation of formic acid have been obtained from premixed flames. Gaydon and Wolfhard [25] conducted a spectroscopic study of low-pressure formic acid / oxygen flames. They found that these flames could be stabilized at pressures as low as 9 torr. The emission spectrum showed the presence of CO and OH in the flames, while CH, C_2, and HCO were not detected. Later, de Wilde and van Tiggelen [26] measured the laminar burning velocity for a wide range of $HOCHO/O_2/N_2$ flames. These data constitute to our knowledge the only quantitative results on the oxidation of formic acid.

The objective of the present study is to develop a detailed chemical kinetic model for oxidation of HOCHO at elevated temperatures, based on ab initio calculations for key consumption reactions of HOCHO, together with the best available thermodynamic data and rate constants from the literature. The resulting model is evaluated by comparing predictions with the available experimental results and used to analyze HOCHO oxidation pathways and rate limiting steps at high temperatures.

Detailed Kinetic Model

In the present study, the starting mechanism and corresponding thermodynamic properties were drawn from recent work by the authors on oxidation of H_2, CO and C_1/C_2 hydrocarbons [27–30]. Both the thermochemistry and the HOCHO oxidation subset of the mechanism were carefully updated. The thermodynamic properties for selected species are shown in Table 1. The data for HOCHO are well established [31], while the properties for HOCO and OCHO have been in question. For HOCO, we rely on the present on-line recommendation of Goos, Ruscic, and Burcat, obtained using the Active Thermochemical Tables (ATcT) approach [33,34], while for OCHO properties were drawn from the theoretical study by Fabian and Janoschek [32]. Compared to the values used by Battin-Leclerc et al. [9], the heats of formation of HOCO and OCHO are smaller by 3 and 23 kJ mol^{-1}, respectively.

Table 2 lists the key reactions in the HOCHO oxidation scheme with the rate coefficients used in the present work. The full mechanism is available as supplemental material. Our subset for HOCHO oxidation is quite different

from those proposed by Marinov [10], Fisher et al. [7] and Battin-Leclerc et al. [9]. Marinov estimated rate constants for reactions of formic acid with O/H radicals by analogy to reactions of CH_3CHO and CH_3OH. He assumed that HOCO and OCHO dissociated instantaneously to form CO + OH and CO_2 + H, respectively. Fisher et al. adopted the HOCHO subset of Marinov, adding a few further reactions with estimated rates. Battin-Leclerc et al. introduced HOCO and OCHO as intermediates in HOCHO oxidation, but employed a reduced reaction subset including only thermal dissociation of HOCHO and HOCHO + OH. In the present work, we characterize the key reactions of HOCHO by ab initio calculations and supplement them with theoretical work from the literature on reactions of HOCO.

Ab initio calculations

Most reactions of HOCHO with the radical pool have not previously been characterized experimentally or theoretically. In this work we have conducted ab initio calculations for reaction of HOCHO with H, O and HO_2. Energies of molecules and transition states were computed at the W1Usc level of theory [45], implemented in the Gaussian 09 program [46]. This is a composite method where the first step is optimization of the geometry at the B3LYP/cc-pV(T+d)Z level of theory, followed by a series of steps that are combined to approximate a coupled-cluster CCSD(T) calculation at the complete-basis set limit, with all electrons correlated and with scalar relativistic (DKH) corrections. The root-mean-square energy error for a range of test systems is 2.4 kJ mol^{-1} [45]. To this we added empirical vector relativistic (spin-orbit) corrections for O atoms and OH radicals of -0.93 and -0.83 kJ mol^{-1}, respectively [47]. These data were used to derive relative enthalpies at 0 K, and

also rate constants via canonical transition state theory. We employed the Multiwell code [48], which allows for approximate Eckart quantum mechanical tunneling corrections and treatment of torsional modes (as determined by visualizing the molecular vibrations) as one-dimensional hindered rotors. The tunneling factor relies on the imaginary frequency at the transition state that corresponds to motion along the reaction coordinate, Because B3LYP is not very accurate for barrier heights [49], we obtained more accurate imaginary frequencies at the M06-2X/cc-pV(T+d)Z level of theory (scaled by a factor of 0.946 [50]). For two test systems, H + CH_2O and H + H_2O, which are simple models for attack at the aldehyde and hydroxyl groups in formic acid, we confirmed the superior performance of the M06-2X functional for the imaginary frequency by comparison with CCSD(T)/cc-pV(T+d)Z data.

The geometries and frequencies of formic acid and the transition states for its abstraction reactions with O, HO_2 and H are listed in the supplemental material. The potential energy diagram for the HOCHO + O reaction is shown in Fig. 1 where it may be seen that attack at the weaker C-H bond to form HOCO (R5) is favored over attack at the stronger O-H bond to form OCHO (R6). In principle, O atoms could add to formic acid to yield triplet diradical species. However, diradicals are not very stable and so are not included in Fig. 1. Addition of O to the O atom in C=O makes triplet H(HO)COO which is, at the CCSD(T)/cc-pVTZ level of theory, 203 kJ mol^{-1} above O + HCOOH and therefore inaccessible. Addition of O to the C of C=O is 46 kJ mol^{-1} endothermic so this diradical is thermodynamically unfavorable under all conditions. Because it is a triplet, dissociation to H_2O + CO_2 is spin-forbidden, but it might make OH + OCHO. The barrier to initial O-atom addition is 79 kJ mol^{-1} so this is effectively a much slower path to the same

products as the direct reaction via TS2.

Figure 2 shows the potential energy diagram for the HOCHO + HO_2 reaction (R9, R10). HO_2 can orient to formic acid to make a seven-membered ring with two strong hydrogen bonds [51], that together add up to a binding energy in the adduct of 55 kJ mol^{-1}. At room temperature and below this will be an important feature of the kinetics, but as the temperature is raised the stability of the adduct decreases, and from the equilibrium constant for adduct formation [51] we estimate that at 400 K, even with 1 atm partial pressure of formic acid, less than 3% of any HO_2 radicals would be complexed. Thus at the conditions relevant here, T > 700 K, this adduct may be neglected. In general, at low temperatures we might expect the oxygen-containing species here to be stabilized by hydrogen bonding to water or formic acid, which may lead to enhanced reactivity under conditions associated with atmospheric chemistry [52, 53], but these interactions will likely not be important under combustion conditions and so are not considered further here. The reaction of HO_2 with CH_2O proceeds via reversible addition across the C=O group, with no overall barrier, to yield $HOCH_2OO$ [55]. The analogous path here has a barrier of 36 kJ mol^{-1}. The two direct abstraction pathways via TS12 and TS13 again favor the more exothermic channel, to HOCO. Because the $H(OH)_2COO$ adduct will only be stable at low temperatures, it will not contribute to our high-temperature systems. In future work we would like to characterize the various addition pathways more quantitatively in case there are any subsequent steps of significance, especially for atmospheric chemistry. Such steps would have to be extremely fast to compensate for the small adduct concentrations expected above 400 K in any high temperature systems (none of which have been investigated experimentally to date).

Possible reactions of formic acid with H atoms are summarized in Fig. 3. The lowest barrier path at 43 kJ mol^{-1} is via TS3 to make $H_2C(O)OH$, which is the intermediate along the path of formic acid formation from OH + CH_2O. Because this intermediate is not thermodynamically stable, and its fastest decomposition path is back to H + HOCHO, we do not consider it further. TS4 at 44 kJ mol^{-1} corresponds to the direct abstraction HOCHO + H $\rightleftharpoons$ HOCO + H_2 (R3) and will be the dominant product channel. The alternative abstraction reaction HOCHO + H $\rightleftharpoons$ OCHO + H_2 (R4) will be substantially slower because TS6 lies 73 kJ mol^{-1} above the reactants. Addition of H to the carbonyl O atom via TS5 (54 kJ mol^{-1}) leads to the most stable $C/H_3/O_2$ isomer, dihydroxymethyl, which lies 43 kJ mol^{-1} below the reactants. This is insufficient to make $HC(OH)_2$ stable at high temperatures, and we do not consider it further here, except to note that it might play a role if it is removed by further rapid chemistry, possibly reaction with O_2. While this paper was under review the two adducts $H_2C(O)OH$ and $HC(OH)_2$ were identified as products of the photolysis of HOCHO/HBr mixtures in a frozen krypton matrix [54].

Reaction mechanism

In addition to the reactions with H, O, and HO_2 discussed above, important consumption steps of HOCHO include thermal dissociation and reaction with OH. The thermal decomposition of HOCHO has been characterized in batch reactor and flow reactor experiments at intermediate temperatures, and in shock tubes at high temperatures. Blake and Hinshelwood [18] conducted batch reactor experiments in the 709-805 K range, measuring CO and CO_2 as function of time. Later, Blake et al. [19] combined batch and flow reac-

tor experiments and extended the temperature range to cover 730-1053 K. The shock tube experiments conducted by Hsu et al. [20] and by Saito and coworkers [21, 22] covered temperatures from about 1300 K to above 2000 K. The thermal dissociation of HOCHO is unusual in that its two product channels yield only stable species, either CO + H_2O (+M) (R1) or H_2 + CO_2 (+M) (R2). The absence of radical producing dissociation channels has been confirmed by Klatt et al. [23] in shock tube experiments at temperatures up to 2450 K and in a number of theoretical studies [35, 56–58]. For the present purposes, the rate constants were drawn from the theoretical work of Chang et al. [35], which is in good agreement with most available experimental data.

The only reaction of formic acid with the O/H radical pool that has been studied experimentally is HOCHO + OH. The reported rate constants, all obtained at low temperatures, are in good agreement, indicating an overall value of $2.7 \cdot 10^{11}$ cm^3 mol^{-1} s^{-1} [59]. The data of Wine et al. [60] and Singleton et al. [59] indicate that the rate constant is independent of temperature in the 297-445 K range. Similar to the other reactions of HOCHO with the radical pool, it has two product channels, HOCO + H_2O (R7) and OCHO + H_2O (R8). The experimental results, including isotopic substitution, indicate that the hydroxyl radical at low temperatures abstracts predominantly the acidic hydrogen. This finding is unexpected because for HOCHO the bond strength of C–H is smaller than that of O–H [36]. Two theoretical studies [36, 61] both indicate that (R8) dominates at room temperature, while (R7) becomes increasingly important at higher temperatures. Anglada [36] calculated rate constants for (R7) and (R8) at temperatures up to 460 K, and we fitted his results to the form $AT^{\beta}exp(-B/T)$ for extrapolation to higher temperatures.

The HOCO radical is an important intermediate in formic acid oxidation. This radical has two stable conformers: trans- and cis-HOCO, with trans-HOCO being more stable by about 7.5 kJ mol^{-1} [62]. In the present work, we do not distinguish between these two conformers. Thermal dissociation of HOCO may yield CO + OH (+M) (R13b) or CO_2 + H (+M) (R14). The behavior of the CO + OH reaction is of both practical and theoretical interest, and a number of experimental and high level ab initio studies have been reported on the CO + OH $\rightleftharpoons$ (HOCO $\rightarrow$) CO_2 + H system. We have adopted the rate constant for (R13) from the theoretical study of Senosiain et al. [38], while k_{14} was drawn from the work of Golden et al. [39]. Modeling predictions are very sensitive to the rate of the HOCO dissociation channels, and an accurate determination of particularly k_{14} is desirable.

The HOCO radical is very reactive towards other small radicals, with rate constants generally in the range of $6 \cdot 10^{12} - 6 \cdot 10^{13}$ cm^3 mol^{-1} s^{-1} [62]. HOCO acts as a hydrogen donor to reaction partners. The mechanism by which the hydrogen is transferred is generally through the formation of an association intermediate, which then proceeds through a molecular elimination step to produce the reaction products [62]. Reactions with the O/H radical pool include reactions (R15)-(R20). None of these reactions have been characterized experimentally. The rate constants were mostly taken from recent high level ab initio work of Francisco, Muckerman, and Yu [37, 40–42, 44]. For the rate constant of the reaction HOCO + OH $\rightleftharpoons$ CO + H_2O_2 (R19b), we rely on own recent work [43].

At the elevated temperatures characteristic of combustion, the HOCO radical dissociates easily (R13b). Under these conditions, only reaction with O_2,

$HOCO + O_2 \rightleftharpoons CO_2 + HO_2$ (R21), may be expected to be competitive. The rate constant for this reaction has been measured at room temperature by Petty et al. [63] and by Nolte et al. [64] to be approximately 10^{12} cm^3 mol^{-1} s^{-1}. Yu et al. [44] calculated a rate constant for the 200-1000 K range in good agreement with the experimental results.

Less is known about the reactions of OCHO. However, the barrier for the exothermic decomposition to CO_2 is no more than a few kcal mol^{-1} and we estimate OCHO to have a lifetime of the order of 10^{-10} s. Consequently, OCHO dissociates rapidly (R22) and is unlikely to react with other species. Even a reaction with O_2 (R24) with an assumed rate constant close to collision frequency is not competitive.

Results and Discussion

To evaluate the model, we have compared predictions to the available quantitative experimental data for oxidation of formic acid at elevated temperatures; that is, the flame speed data from de Wilde and van Tiggelen [26]. Data on the pyrolysis of formic acid have not been included in the analysis. We expect these data to provide information only on the thermal dissociation of HOCHO (R1, R2), which seems to be well established. Bone and Gardner [24] reported that oxidation of formic acid in a static reactor (613-743 K, atmospheric pressure) was significantly slower than oxidation of CH_4, CH_3OH and CH_2O but offered no quantitative data.

De Wilde and van Tiggelen [26] conducted a comparative experimental study of flames propagating in mixtures of oxygen with methanol, formaldehyde,

and formic acid. The flame speed of HOCHO was shown to be significantly lower than those of methanol or formaldehyde, even though a direct comparison was not possible since the latter flames were operated at higher dilution levels. As the heat of combustion of formic acid is low, flames were propagating only in $HOCHO/O_2/N_2$ mixtures with a smaller amount of N_2 compared to HOCHO/air mixtures. De Wilde and van Tiggelen investigated mixtures with 12–24% N_2 and fuel/air equivalence ratios in the range 0.4–1.2. The experiments were conducted with an inlet flow temperature of 433 K.

Figure 4 compares the measured flame speeds of formic acid reported by de Wilde and van Tiggelen for mixtures with 12%, 18%, and 24% N_2 as a function of fuel/air equivalence ratio with model predictions from the present work. An unusual feature of the formic acid flames is that the burning velocity peaks at lean conditions ($\phi \approx 0.8$), corresponding to the stoichiometry where also the flame temperature reaches its maximum [26].

The modeling predictions agree satisfactorily with the observed flame speeds. For the least diluted flame (12% N_2), the measured flame speed is predicted quite accurately by the model over the range of stoichiometries. As the dilution increases and flame temperatures decrease, differences between observed and predicted values become larger, with the 24% N_2 flame speeds being overpredicted by 5-15 cm s^{-1}. These discrepancies can partly be attributed to experimental uncertainties, but uncertainties in the rate constants for some of the key reactions in the mechanism, in particular those important for the fate of HOCO, are likely to contribute.

A pathway analysis of the flame calculations reveals the major oxidation pathways for formic acid. Formic acid is mainly consumed by reaction with

OH to form OCHO + H_2O (R8) and HOCO + H_2O (R7), and by HO_2, HOCHO + $HO_2 \rightleftharpoons$ HOCO + H_2O_2 (R9). The reaction with HO_2 (R9) is most significant in the low-temperature, early part of the flame. The OCHO radical formed in reaction (R8) dissociates rapidly to yield CO_2 + H (R22).

The HOCO radical dissociates thermally at higher temperatures, mainly through HOCO (+M) $\rightleftharpoons$ CO + OH(+M) (R13b), while in the low-temperature regions of the flame it reacts predominantly with O_2, HOCO + $O_2 \rightleftharpoons$ CO_2 + HO_2 (R21). Minor consumption steps in the cooler part of the flame include the reactions with HO_2, HOCO + $HO_2 \rightleftharpoons$ CO_2 + H_2O_2 (R20), and with H_2 diffusing upstream in the flame, HOCO + $H_2 \rightleftharpoons$ HOCHO + H (R3b).

Figure 5 shows the sensitivity of the predicted flame speed at a fuel/air equivalence ratio ϕ of 0.8 and a N_2 dilution of 18% towards key reactions in the HOCHO subset. The calculated flame speed is very sensitive to the competition between generation and consumption of chain carriers. The largest positive sensitivity coefficients are found for the reaction of HOCHO with OH to form OCHO+H_2O (R8), which is followed by rapid dissociation of OCHO to form CO_2 and H (R22), and for thermal dissociation of HOCO (R13b and R14). The largest negative sensitivity coefficients are found for the reactions of HOCO with H (R15), OH (R18), and O_2 (R21). By competing with the thermal dissociation of HOCO, these steps are effectively chain terminating and serve to slow down the burning velocity.

Conclusions

A reaction mechanism for oxidation of HOCHO at intermediate and high temperatures has been developed. Ab initio calculations were used to obtain

rate coefficients for reactions of HOCHO with H, O, and HO_2. Modeling predictions with the mechanism were in satisfactory agreement with measured laminar burning velocities of HOCHO. In the flames, formic acid is consumed mainly by reaction with OH, yielding OCHO, which dissociates rapidly to CO_2 + H, and HOCO, which may dissociate to CO + OH or CO_2 + H, or react with H, OH, or O_2 to form more stable products. The branching fraction of the HOCHO + OH reaction, as well as the fate of HOCO, determines the oxidation rate of formic acid.

Acknowledgements

This work was supported by the R.A. Welch Foundation (Grant B-1174) and computational facilities were supported in part by the National Science Foundation (Grant CHE-0741936).

References

[1] J.E. Lawrence, P. Koutrakis, Environ. Sci. Technol. 28 (1994) 957-964.

[2] A. Chebbi, P. Carlier, Atmos. Environ. 30 (1996) 4233-4249.

[3] E. Zervas, X. Montagne, J. Lahaye, Atmos Environ 35 (2001) 1301-1306.

[4] E. Zervas, X. Montagne, J. Lahaye, Environ Sci Technol 35 (2001) 2746-2751.

[5] E. Biagini, F. Barontini, L. Tognotti, Ind. Eng. Chem. Res. 45 (2006) 4486-4493.

[6] T.J. Held, F.L. Dryer, Int. J. Chem. Kinet. 30 (1998) 805-830.

[7] S.L. Fischer, F.L. Dryer, H.J. Curran, Int. J. Chem. Kinet. 32 (2000) 713-740.

[8] E. Zervas, Fuel 84 (2005) 691-700.

[9] F. Battin-Leclerc, A.A. Konnov, J.L. Jaffrezo, M. Legrand, Combust. Sci. Technol. 180 (2007) 343-370.

[10] N.M. Marinov, Int. J. Chem. Kinet. 31 (1999) 183-220.

[11] P.H. Taylor, M.S. Rahman, M. Arif, B. Dellinger, P. Marshall, Proc. Combust. Inst. 26 (1996) 497-504.

[12] M.U. Alzueta, M. Borruey, A. Callejas, A. Millera, R. Bilbao, Combust. Flame 152 (2008) 377-386.

[13] S. Hatakeyama, N. Washida, H. Akimoto, J. Phys. Chem. 90 (1986) 173-178.

[14] B. Bohn, C. Zetzsch, Phys. Chem. Chem. Phys. 1 (1999) 5097-5107.

[15] A. Maranzana, J.R. Barker, G. Tonachini, J. Chem. Phys. A 112 (2008) 3666-3675.

[16] A. Galano, L.G. Ruiz-Suarez, A. Vivier-Bunge, Theor. Chem. Account 121 (2008) 219-225.

[17] D.R. Glowacki, M.J. Pilling, ChemPhysChem 11 (2010) 3836-3843.

[18] P.G. Blake, C. Hinshelwood, Proc. R. Soc. Lond. A 255 (1960) 444-455.

[19] P.G. Blake, H.H. Davies, G.E. Jackson, J. Chem. Soc. B 10 (1971) 1923-1925.

[20] D.S.U. Lin, W.M. Shaub, M. Blackburn, M.C. Lin, Proc. Combust. Inst. 19 (1982) 89-96.

[21] K. Saito, T. Kakumoto, H. Kuroda, A. Imamura, J. Chem Phys 80 (1984) 4989-4996.

[22] K. Saito, T. Shiose, O. Takahashi, Y. Hidaka, F. Aiba, K. Tabayashi, J. Phys. Chem. A 109 (2005) 5352-5357.

[23] M. Klatt, M. Röhrig, H.Gg. Wagner, Z. Naturforsch. 47 (1992) 1138-1140.

[24] W.A. Bone, J.B. Gardner, Proc. R. Soc. Lond. A 154 (1936) 297-328.

[25] A.G. Gaydon, H.G. Wolfhard, Third Symp. Combust. Flame Explos. Phenom. 504-518 (1949).

[26] E. de Wilde, A. van Tiggelen, Bull. Soc. Chim. Belges 77 (1968) 67-76.

[27] H. Hashemi, J.M. Christensen, S. Gersen, P. Glarborg, "Hydrogen Oxidation at High Pressure and Intermediate Temperatures: Experiments and Kinetic Modeling", 35^{th} Symp. (Int.) Combust., accepted for presentation (2014).

[28] C.L. Rasmussen, J. Hansen, P. Marshall, P. Glarborg, Int. J. Chem. Kinet. 40 (2008) 454-480.

[29] C.L. Rasmussen, J.G. Jacobsen, P. Glarborg, Int. J. Chem. Kinet. 40 (2008) 778-807.

[30] J. Gimenez, C.L. Rasmussen, M.U. Alzueta, P. Marshall, P. Glarborg, Proc. Combust. Inst. 32 (2009) 367-375.

[31] A. Burcat, B. Ruscic, "*Third Millennium Ideal Gas and Condensed Phase Thermochemical Database for Combustion with Updates from Active Thermochemical Tables*", Report TAE960, Technion Israel Inst. of Technology, 16th September 2005.

[32] W.M.F. Fabian, R.J. Janoschek, Mol. Struct. THEOCHEM 713 (2008) 227-234.

[33] B. Ruscic, R.E. Pinzon, M.L. Morton, G. von Laszewski, S. Bittner, S.G. Nijsure, K.A. Amin, M. Minkoff, A.F. Wagner, J. Phys. Chem. A 108 (2004) 9979-9997.

[34] B. Ruscic, R.E. Pinzon, G. von Laszewski, D. Kodeboyina, A. Burcat, D. Leahy, D. Montoya, A.F. Wagner, J. Phys. Conf. Ser. 16 (2005) 561-570.

[35] J.-G. Chang, H.-T. Chen, S. Xu, M.C. Lin, J. Phys. Chem. A 111 (2007) 6789-6797.

[36] J.M. Anglada, J. Am. Chem. Soc. 126 (2004) 9809-9820.

[37] H.G. Yu, G. Poggi, J.S. Francisco, J.T. Muckerman, J. Chem. Phys. 129 (2008) 214307.

[38] J.P. Senosiain, S.J. Klippenstein, J.A. Miller, Proc. Combust. Inst. 30 (2005) 945-953.

[39] D.M. Golden, G.P. Smith, A.B. McEwen, C.-L. Yu, B. Eiteneer, M. Frenklach, G.L. Vaghjiani, A.R. Ravishankara, F.P. Tully, J. Phys. Chem. A 102 (1998) 8598-8606.

[40] H.G. Yu, J.S. Francisco, J. Chem. Phys. 128 (2008) 244315.

[41] H.G. Yu, J.T. Muckerman, J.S. Francisco, J. Chem. Phys. 127 (2007) 094302.

[42] H.G. Yu, J.T. Muckerman, J.S. Francisco, J. Phys. Chem. A 109 (2005) 5230-5236.

[43] P. Glarborg, P. Marshall, Chem. Phys. Lett. 475 (2009) 40-43.

[44] H.G. Yu, J.T. Muckerman, J. Phys. Chem. A 110 (2006) 5312-5316.

[45] E.C. Barnes, G.A. Petersson, J.A. Montgomery, Jr., M.J. Frisch, J.M.L. Martin, J. Chem. Theory Comput. 5 (2009) 2687-2693.

[46] M.J. Frisch et al., Gaussian 09 (Gaussian, Wallingford CT, 2010).

[47] NIST Computational Chemistry Comparison and Benchmark Database, NIST Standard Reference Database Number 101 , Release 16a, August 2013, Editor: Russell D. Johnson III (http://cccbdb.nist.gov).

[48] MultiWell-2012.2, 2012, J.R. Barker, N.F. Ortiz, J.M. Preses, L.L. Lohr, A. Maranzana, P.J. Stimac, T.L. Nguyen, T.J.D. Kumar; University of Michigan, Ann Arbor, MI; http://aoss.engin.umich.edu/multiwell/.

[49] J. Zheng, Y. Zhao, D.G. Truhlar, J. Chem. Theory Comput. 5 (2009) 808-821.

[50] I.M. Alecu, J. Zheng, Y. Zhao, D.G. Truhlar, J. Chem. Theory Comput. 6 (2010) 2872-2887.

[51] S. Aloisio and J.S. Francisco, J. Am. Chem. Soc. 122 (2000) 9196-9200.

[52] S. Aloisio and J.S. Francisco, Acc. Chem. Res. 33 (2000) 825-830.

[53] M.K. Hazra, J.S. Francisco and A. Sinha, J. Phys. Chem. A 117 (2013) 11704-11710.

[54] Q. Cao, S. Berski, Z. Latajka, M. Rasanen and L. Khriachtchev, Phys. Chem. Chem. Phys. 16 (2014) 5993-6001

[55] J.M. Anglada and V.M. Domingo, J. Phys. Chem. A 109 (2005) 10786-10794.

[56] J.S. Francisco, J. Chem. Phys. 96 (1992) 1167-1175.

[57] I.V. Tokmakov, C.C. Hsu, L.V. Moskaleva, M.C. Lin, Mol. Phys. 92 (1997) 581-586.

[58] N. Akiy, P.E. Savage, AIChE J. 44 (1998) 405-415.

[59] D.L. Singleton, G. Paraskevopoulos, R.S. Irwin, G.S. Jolly, D.J. McKenney, J. Am. Chem. Soc. 110 (1988) 7786-7790.

[60] P.H. Wine, R.J. Astalos, R.L. Mauldin, III., J. Phys. Chem. 89 (1985) 2620-2624.

[61] A. Galano, J.R. Alvarez-Idaboy, Ma.E. Ruiz-Santoyo, A. Vivier-Bunge, J. Phys. Chem. A 106 (2002) 9520-9528.

[62] J.S. Francisco, J.T. Muckerman, H.G. Yu, Accounts Chem. Res. 43 (2010) 1519-1526.

[63] J.T. Petty, J.A. Harrison, C.B. Moore, J. Phys. Chem. 97 (1993) 11194-11198.

[64] J. Nolte, J. Grussdorf, F. Temps, H.Gg. Wagner, Z. Naturforsch. A 48 (1993) 1234-1238.

[65] R. Atkinson, D.L. Baulch, R.A. Cox, R.F. Hampson, Jr., J.A. Kerr, M.J. Rossi, J. Troe, J. Phys. Chem. Ref. Data 26 (1997) 521-1011.

[66] G.S. Jolly, D.J. McKenney, D.L. Singleton, G. Paraskevopoulos, A.R. Bossard, J. Phys. Chem. 90 (1986) 6557-6562.

Species	H_{298}	S_{298}	$C_{p,300}$	$C_{p,400}$	$C_{p,500}$	$C_{p,600}$	$C_{p,800}$	$C_{p,1000}$	$C_{p,1500}$	Ref.
HOCHO	-378.8	247.3	41.45	48.15	54.81	60.71	69.38	75.87	85.37	[31]
HOCO	-184.1	251.8	43.75	49.45	54.39	58.53	64.44	68.62	74.57	see text
OCHO	-127.5	256.5	48.78	53.93	58.49	62.34	68.25	72.18	77.54	[32]

Table 1: Thermodynamic properties of selected species in the reaction mechanism. Units are kJ mol^{-1} for H, and J mol^{-1} K^{-1} for S and C_p. Temperature (T) range is in K.

		A [cm,mole,s]	β	E_a/R [K]	Source
1.	$HOCHO(+M) \rightleftharpoons CO + H_2O(+M)$	7.5E14	0.000	34580	[35]
	Low pressure limit:	4.1E15	0.000	26660	
2.	$HOCHO(+M) \rightleftharpoons CO_2 + H_2(+M)$	4.5E13	0.000	34340	[35]
	Low pressure limit:	1.7E15	0.000	25720	
3.	$HOCHO + H \rightleftharpoons HOCO + H_2$	2.3E02	3.272	2445	pw
4.	$HOCHO + H \rightleftharpoons OCHO + H_2$	4.2E05	2.255	7092	pw
5.	$HOCHO + O \rightleftharpoons HOCO + OH$	5.1E01	3.422	2122	pw
6.	$HOCHO + O \rightleftharpoons OCHO + OH$	1.7E05	2.103	4972	pw
7.	$HOCHO + OH \rightleftharpoons HOCO + H_2O$	7.8E-6	5.570	-1190	[36][a]
8.	$HOCHO + OH \rightleftharpoons OCHO + H_2O$	4.9E-5	4.910	-2550	[36][a]
9.	$HOCHO + HO_2 \rightleftharpoons HOCO + H_2O_2$	4.7E-1	3.975	8448	pw
10.	$HOCHO + HO_2 \rightleftharpoons OCHO + H_2O_2$	3.9E01	3.080	12685	pw
11.	$HOCO + HO_2 \rightleftharpoons HOCHO + O_2$	4.0E11	0.000	0	[37]
12.	$HOCHO + O_2 \rightleftharpoons OCHO + H_2O_2$	3.0E13	0.000	31700	est
13.	$CO + OH \rightleftharpoons HOCO$	2.0E20	-3.500	659	1.0 bar, [38]
14.	$HOCO(+M) \rightleftharpoons CO_2 + H(+M)$[b]	8.2E11	0.413	35335	[39]
	Low pressure limit:	6.0E26	-3.148	37116	
15.	$HOCO + H \rightleftharpoons CO_2 + H_2$	3.1E17	-1.3475	279	[40][a]
16.	$HOCO + H \rightleftharpoons CO + H_2O$	6.0E15	-0.525	1069	[40][a]
17.	$HOCO + O \rightleftharpoons CO_2 + OH$	9.0E12	0.000	0	[41]
18.	$HOCO + OH \rightleftharpoons CO_2 + H_2O$	4.6E12	0.000	-45	[28, 42][c]
		9.5E06	2.000	-45	
19.	$CO + H_2O_2 \rightleftharpoons HOCO + OH$	3.6E04	2.500	14424	[43]
20.	$HOCO + HO_2 \rightleftharpoons CO_2 + H_2O_2$	4.0E13	0.000	0	[37]
21.	$HOCO + O_2 \rightleftharpoons CO_2 + HO_2$	4.0E09	1.000	0	[44][a]
22.	$OCHO \rightleftharpoons CO_2 + H$	1.0E10	0.000	0	est
23.	$OCHO + O_2 \rightleftharpoons CO_2 + HO_2$	5.0E13	0.000	0	est

a: Rate coefficients fitted to data reported.

b: Troe fall-off parameters: $F_c = 0.39$.

c: Expressed as the sum of the rate constants at a given pressure.

Table 2: Reaction subset for formic acid oxidation. Parameters for use in the modified Arrhenius expression $k = AT^{\beta}\exp(-E/[RT])$. Units are mol, cm, s, K.

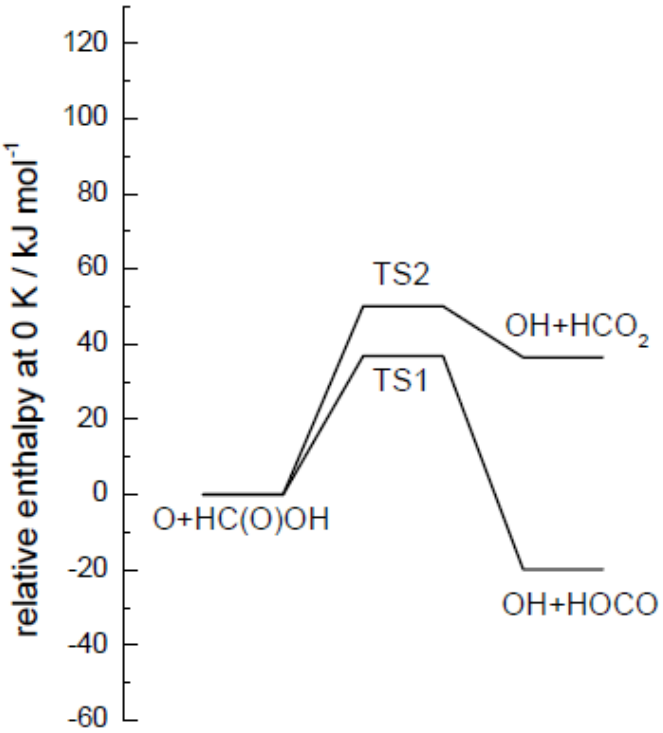

Figure 1: Relative enthalpies computed for 0 K based on W1U energies for the HOCHO + O reaction system.

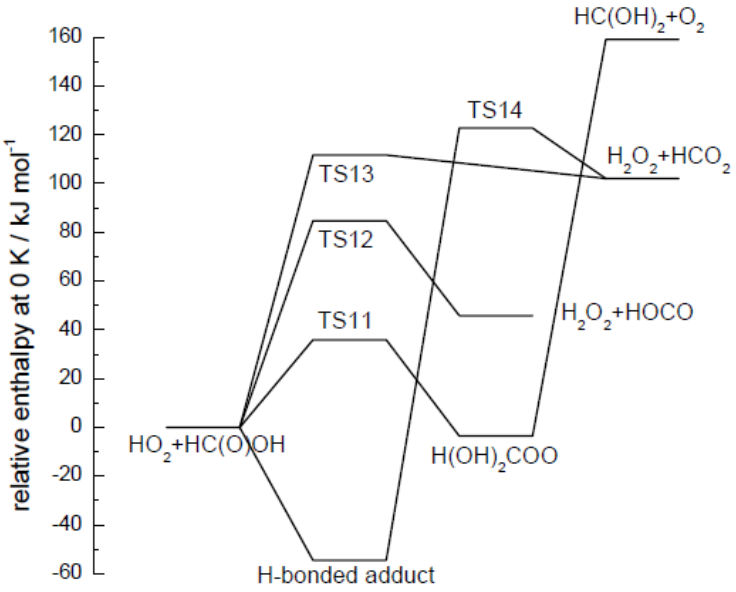

Figure 2: Relative enthalpies computed for 0 K based on W1U energies for the HOCHO + HO_2 reaction system.

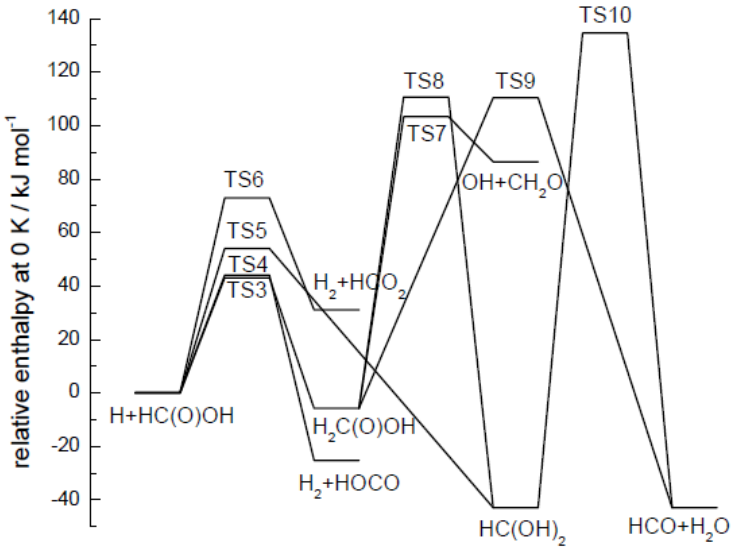

Figure 3: Relative enthalpies computed for 0 K based on W1U energies for the HOCHO + H reaction system.

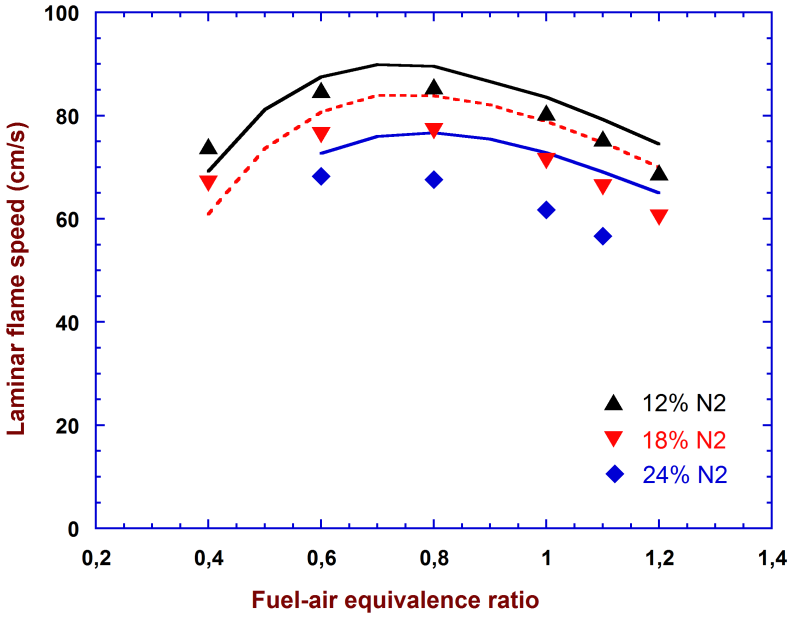

Figure 4: Comparison of experimental and predicted flame speeds for HO-CHO / O_2 / N_2 for an initial temperature of 433 K as a function of fuel-air equivalence ratio and N_2 dilution. The symbols mark the experimental data from De Wilde and van Tiggelen [26] while lines denote model predictions. In the tabulation of de Wilde and van Tiggelen, values were corrected to room temperature, but the figure shows the uncorrected values corresponding to the 433 K inlet temperature.

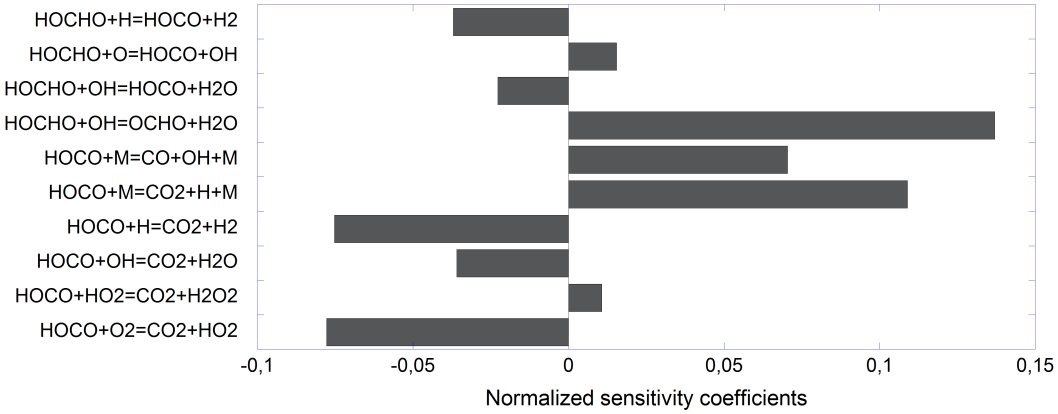

Figure 5: Sensitivity coefficients for the predicted flame speed for HOCHO / O_2 / N_2 at $\phi = 0.8$, 18% N_2, and an inlet gas temperature of 433 K. Only coefficients for key reactions in the HOCHO subset of the mechanism are shown.